

1 **Title:** High throughput screening of Leaf Economics traits in six wine grape varieties

2

3 **Running Title:** Spectral reflectance and leaf economics in wine grapes

4

5 **Authors Information:** Boya Cui <sup>1</sup>, Rachel Mariani <sup>1</sup>, Kimberley A. Cathline <sup>2</sup>, and Gavin  
6 Robertson <sup>2</sup>, Adam R. Martin <sup>1,\*</sup>

7

8 <sup>1</sup> Department of Physical and Environmental Sciences, University of Toronto Scarborough,  
9 Canada

10 <sup>2</sup> Horticultural & Environmental Sciences Innovation Centre, Niagara College, Canada

11 \*Corresponding author: [adam.martin@utoronto.ca](mailto:adam.martin@utoronto.ca)

12

13 **Keywords:** Agroecology, crop trait, functional trait, high throughput phenotyping, reflectance  
14 spectroscopy.

15

## 16 **Abstract**

17 Reflectance spectroscopy has become a powerful tool for non-destructive and high-  
18 throughput phenotyping in crops. Emerging evidence indicates that this technique allows for  
19 estimation of multiple leaf traits across large numbers of samples, while alleviating the  
20 constraints associated with traditional field- or lab-based approaches. While the ability of  
21 reflectance spectroscopy to predict leaf traits across species and ecosystems has received  
22 considerable attention, whether or not this technique can be applied to quantify within species  
23 trait variation have not been extensively explored. Employing reflectance spectroscopy to  
24 quantify intraspecific variation in functional traits is especially appealing in the field of  
25 agroecology, where it may present an approach for better understanding crop performance,  
26 fitness, and trait-based responses to managed and unmanaged environmental conditions. We  
27 tested if reflectance spectroscopy coupled with Partial Least Square Regression (PLSR) predicts  
28 rates of photosynthetic carbon assimilation ( $A_{\max}$ ), Rubisco carboxylation ( $V_{\text{cmax}}$ ), electron  
29 transport ( $J_{\max}$ ), leaf mass per area (LMA), and leaf nitrogen (N), across six wine grape (*Vitis*  
30 *vinifera*) varieties (Cabernet Franc, Cabernet Sauvignon, Merlot, Pinot Noir, Viognier,  
31 Sauvignon Blanc). Our PLSR models showed strong capability in predicting intraspecific trait

32 variation, explaining 55%, 58%, 62%, and 64% of the variation in observed  $J_{\max}$ ,  $V_{\max}$ , leaf N,  
33 and LMA values, respectively. However, predictions of  $A_{\max}$  were less strong, with reflectance  
34 spectra explaining only 29% of the variation in this trait. Our results indicate that trait variation  
35 within species and crops is less well-predicted by reflectance spectroscopy, than trait variation  
36 that exists among species. However, our results indicate that reflectance spectroscopy still  
37 presents a viable technique for quantifying trait variation and plant responses to environmental  
38 change in agroecosystems.

39

## 40 **Introduction**

41 Plant functional traits refer to the morphological, physiological, or phenological  
42 characteristics of plants that are readily measurable at an organismal scale, and influence the  
43 performance and response of individuals to environmental changes [1-4]. A considerable amount  
44 of effort has been directed towards understanding the extent, causes, and consequences of trait  
45 variation among plant species [5-10]. This body of literature has led to a deeper understanding of  
46 the key dimensions of functional trait variation that exist among the world's plant species [6, 11].

47 Among the most well-studied dimensions of trait variation employed to describe and  
48 predict plant performance across resource availability gradients, is the “Leaf Economics  
49 Spectrum” (LES) [7-9]. The LES is a suite of six core leaf traits that covary among plant species  
50 including maximum photosynthetic assimilation ( $A_{\max}$ ), leaf dark respiration rate ( $R_d$ ), leaf  
51 nitrogen (N) and phosphorus (P) concentrations, leaf mass per area (LMA), and leaf lifespan  
52 (LL). Taken together, LES trait expression defines how species vary across a continuum of life-  
53 history strategies, from fast-growing species characterized by rapid return on biomass  
54 investment, low structural investment, high leaf nutrient concentrations, and relatively short  
55 lifespans on one end, to resource-conserving species expressing the opposite suite of traits and  
56 by extension can be more resilient to resource limitation. Variation in LES traits largely owes to  
57 evolved trade-offs related to leaf biomechanics [12, 13], as well as evolved or plastic variation in  
58 physiological and leaf structural traits including stomatal and mesophyll conductance ( $g_s$  and  $g_m$ ,  
59 respectively), which in turn influence rates of maximum Rubisco carboxylation ( $V_{\max}$ ), the  
60 electron transport ( $J_{\max}$ ) [14-16].

61 Although much of the seminal work on trait variation is been based on interspecific  
62 comparisons, more recent research has focused on quantifying the extent and ecological

63 implications of intraspecific trait variation [17-21]. Given the role that phenotypic plasticity and  
64 inheritable genetic variation play in governing plant ecophysiology and morphology, plant  
65 species can exhibit a high degree of intraspecific variation across a range of traits [21] and trait  
66 dimensions [17, 22]. Quantifying intraspecific trait variation is especially critical in  
67 agroecosystems where a relatively small number of plant species drive rates of ecosystem  
68 functioning on account of high abundances [23, 24]. Indeed, considerable interest and efforts  
69 have been dedicated to quantifying the causes and consequences of intraspecific variation in the  
70 traits that are directly responsible for crop growth, survival, and reproduction.

71         Though efforts to comprehensively assess intraspecific trait variation in a given plant  
72 species, especially crops, are often limited at the data collection phase of scientific enquiry.  
73 Traditionally, functional trait data are collected or derived from a combination of field and  
74 laboratory measurements, most of which can be laborious and time-consuming. This is especially  
75 true for “hard” traits [sensu 5] that are part of the LES such as  $A_{\max}$  and  $R_d$  which are generated  
76 through point sampling of photosynthesis using portable infrared gas analyzers. Furthermore,  
77 traits that contribute to the physiological basis of LES trait variation, namely  $V_{\text{cmax}}$  and  $J_{\text{max}}$ , rely  
78 on the execution and analysis of time-consuming photosynthetic  $\text{CO}_2$  response curves ( $A-C_i$ )  
79 [reviewed by 25]. These methodological limitations to trait collection have at least in part  
80 motivated extensive research that evaluates how more easily-measured “soft” traits such as LMA  
81 can be used to predict “hard” physiological traits [5], especially in the context of Earth System  
82 Model parameterization [26, 27].

83         Reflectance spectroscopy has emerged as a central component of high-throughput  
84 phenotype assessments and related collection of physiological, chemical, and morphological trait  
85 data [28]. While multi- and hyperspectral sensors form a key component of remotely-sensed  
86 spectral diversity assessments at ecosystem scales [29-32], field-based reflectance spectroscopy  
87 offers an opportunity to rapidly amass species- or genotype-scale data on leaf physiological,  
88 chemical, and morphological traits including those forming the LES [33-35]. Specifically, using  
89 Partial Least Square Regression (PLSR) models [36], studies have reported strong predictive  
90 relationships between reflectance spectra and LES traits including  $A_{\max}$ , leaf N, LMA, and  
91 related physiological parameters including  $V_{\text{cmax}}$  and  $J_{\text{max}}$  [33, 37-39].

92         Spectroscopy coupled with PLSR models has been successful in estimating plant traits,  
93 particularly when using multi-species datasets that present a wide range of trait values and

94 spectral profiles [33, 38, 40]. More recently, studies have begun employing these techniques to  
95 quantify and predict finer-scale intraspecific trait variation [41], including trait variation across  
96 individuals or genotypes of the same crop species [42-47]. Analyses on intraspecific trait  
97 variation—where trait values and spectra are more constrained—are less common vs. studies  
98 analyzing trait values and spectral signatures from a number of species differing in life-history  
99 strategies [33, 38] or agronomic profiles [40]. Furthermore, studies using reflectance  
100 spectroscopy to detect intraspecific trait variation in crops, commonly screen plants from a range  
101 of managed environmental conditions which further contributes a wider range of trait values  
102 [43]. While these results are promising, there remains uncertainty regarding whether or not these  
103 techniques are able to differentiate LES traits across individuals or genotypes of the same  
104 species, in agroecosystems where environmental conditions are more homogeneous.

105 Our study aims to contribute to the literature on high-throughput assessments of  
106 intraspecific trait variation, by evaluating the potential of reflectance spectroscopy to predict  
107 LES trait variations across multiple wine grape (*Vitis vinifera*) varieties: one of the most  
108 common crops that holds substantial agricultural and economic values. In this study, we hope to  
109 determine whether PLSR models can reliably estimate photosynthetically important functional  
110 traits in wine grapes from reflectance spectroscopy data across six cultivated varieties.

111

## 112 **Materials and Methods**

### 113 *Study site*

114 We collected LES and related trait and spectral reflectance data for six of the most  
115 common wine grape varieties—Cabernet Franc, Cabernet Sauvignon, Merlot, Pinot Noir,  
116 Sauvignon Blanc, Viognier—at the Niagara College Teaching Vineyard, Niagara-on-the-Lake,  
117 Ontario. The site is an operational vineyard characterized as non-irrigated, with imperfectly  
118 drained silty clays overlaying clay loam till mixed with poorly drained lacustrine heavy clay, and  
119 uniformly tilled and sprayed [48, 49]. All trait and reflectance data were collected during the  
120 fruit setting stage (at our site, from June 6-17, 2022) between 6:00-12:00. For each variety, we  
121 sampled 30 vines evenly distributed across three planting rows, which were roughly 10 meters  
122 apart from each other within one row, totalling  $n=180$  individual vines. One leaf on each vine  
123 was selected from the uppermost segment of the individual for data collection, with all leaves  
124 being fully exposed, newly developed, fully expanded, and free of any damage [50].

125

126 *Functional trait data collection*

127 Trait data in our study included  $A_{\max}$ ,  $V_{\text{cmax}}$ , and  $J_{\max}$ , leaf N concentrations, and LMA.  
128 First,  $V_{\text{cmax}}$ ,  $J_{\max}$ , and  $A_{\max}$  data were collected in the field using a LI-6800 Portable  
129 Photosynthesis System (Licor Bioscience, Lincoln, Nebraska, USA). We first performed an  $A-C_i$   
130 curve on each leaf using the Dynamic Assimilation Technique (DAT) [25, 51, 52] in order to  
131 estimate rates of  $V_{\text{cmax}}$  and  $J_{\max}$ . For each curve,  $\text{CO}_2$  assimilation rates on a per leaf area basis  
132 ( $A_{\text{area}}$ ;  $\mu\text{mol CO}_2 \text{ m}^{-2} \text{ s}^{-1}$ ) were logged every 4 seconds across continuously ramping  $\text{CO}_2$   
133 concentrations, with a ramp rate of  $100 \mu\text{mol mol}^{-1} \text{ min}^{-1}$  [consistent with recommendations by  
134 52, 53] beginning at  $5 \mu\text{mol mol}^{-1} \text{ CO}_2$  and concluding at  $1700 \mu\text{mol mol}^{-1} \text{ CO}_2$ . Otherwise,  
135 conditions in the leaf chamber were set to a photosynthetic photon flux density (PPDF) of  $1500$   
136  $\mu\text{mol m}^{-2} \text{ s}^{-1}$  of photosynthetically active radiation (PAR; 400-700 nm), 50% relative humidity,  
137 leaf vapour pressure deficits of 1.7 KPa, and leaf temperatures of 25 °C. Furthermore,  $\text{CO}_2$  and  
138  $\text{H}_2\text{O}$  sensors were readjusted using the range match function after every five leaf measurements,  
139 and each DAT  $A-C_i$  curve required approximately 10 minutes, including a 60-120 second  
140 acclimation period [25]. Following the completion of each  $A-C_i$  curve, we then allowed leaves to  
141 acclimate to ambient conditions for ~10 minutes. Then, we collected steady-state  $A_{\max}$  values for  
142 each leaf at the same environmental conditions as mentioned above with a constant  $\text{CO}_2$   
143 concentration at 420 ppm. We logged steady-state gas  $A_{\max}$  values after leaves were allowed to  
144 stabilize for 5-10 minutes.

145 Immediately following gas exchange measurements, we used an HR1024i full spectrum  
146 portal field spectroradiometer (Spectra Vista Corporation, Poughkeepsie NY, USA) to collect  
147 reflectance spectra for each leaf. This instrument is a full-range spectroradiometer (350-2500  
148 nm) with a spectral resolution of  $\leq 3.5$  nm (350-1000 nm),  $\leq 9.5$  nm (1000-1800 nm), and  $\leq 6.5$   
149 nm (1800-2500 nm), outfitted with an LC-RP Pro leaf clip that includes a calibrated internal light  
150 source. Reflectance spectra were collected at the same location on the adaxial side of each leaf  
151 from which  $A-C_i$  and steady state gas exchange were performed, with integration times set to 2  
152 seconds, and reference spectra taken on a white Spectralon standard prior to each measurement.

153 Once physiological and reflectance data were acquired, we collected and transported  
154 individual leaves to the University of Toronto Scarborough for quantification of LMA and leaf N  
155 concentrations. First, we removed all petioles, and the fresh area of all leaves was quantified

156 using an LI-3100C leaf area meter (Licor Bioscience, Lincoln, Nebraska, USA), and then dried  
157 for 48 hours to constant mass. Dried leaves were then weighed and LMA was calculated as mass/  
158 area. Finally, dried leaves were ground to a fine and homogeneous powder using a MM400  
159 Retsch ball mill (Retsch Ltd., Hann, Germany), and a LECO CN 628 elemental analyzer (LECO  
160 Instruments, Ontario, Canada) was used to determine leaf N concentrations on ~0.1 grams of  
161 powdered tissue.

162

### 163 *Data analysis*

164 R Statistical Software v. 4.2.0 (R Foundations for Statistical Computing, Vienna, Austria)  
165 was used for all data analysis. First, we fit the Farquhar, von Caemmerer and Berry (FvCB)  
166 model to each individual  $A-C_i$  curve, using the ‘fitaci’ function in the ‘plantecophys’ R package  
167 [54], in order to estimate rates of  $V_{\text{cmax}}$  and  $J_{\text{max}}$ , along with their standard errors. In this  
168 procedure, these models were fit using non-linear least square regression [54], such that  $V_{\text{cmax}}$   
169 and  $J_{\text{max}}$  were corrected to 25 °C, and  $V_{\text{cmax}}$  and  $J_{\text{max}}$  are considered apparent as mesophyll  
170 conductance was assumed to be infinite. These data were merged with other traits, and the  
171 distribution of each individual trait was assessed using the ‘fitdist’ function in the ‘fitdistrplus’ R  
172 package [55]. Traits were determined to be either normally or log-normally distributed (as per  
173 the highest log-likelihood value) and transformed data was employed in further analyses in  
174 accordance with these results. We then performed an analysis of variance (ANOVA) to test for  
175 significant trait differences across varieties.

176 We then followed the methods described by Burnett et al. [36] to evaluate how  
177 reflectance spectra predicted trait values across our dataset, using a PLSR modelling approach.  
178 All PLSR models included reflectance spectral data from the 500-2400 nm wavelength range,  
179 and aimed to predict either non-transformed or log-transformed trait data, as informed by our  
180 distribution fitting procedure. For each PLSR model, the spectra-trait dataset was split into a  
181 calibration dataset (which included 80% of all data points) and a validation dataset (comprised of  
182 the remaining 20% of data). Since we were explicitly interested in testing the ability of  
183 reflectance spectra to quantify variation in leaf traits across grapes broadly, and the ability to  
184 differentiate varieties, we performed and analyzed two data splits. First, datasets were split into  
185 calibration vs. validation according to variety identity, such that both the validation and  
186 calibration datasets had approximately equal proportions of trait and spectra data from all

187 varieties. Second, we used a completely randomized data split, whereby the proportion of data  
188 across varieties was allowed to vary randomly.

189 Using the calibration datasets, we then used the ‘find\_optimal\_components’ function in  
190 the ‘spectratrait’ R package [56] to determine the optimal number of components used in the  
191 final PLSR model, based on the minimization of the prediction residual sum of squares (PRESS)  
192 statistic. For each trait, a PLSR model was fitted from the calibration dataset using the leave-one-  
193 out cross-validation (LOO) procedure, specified with the ‘plsr’ function in the ‘pls’ R package  
194 [57]. Model performance was then assessed with the validation datasets as an external validation,  
195 in which the predicted values and the observed values in the validation dataset were compared.  
196 For the final models, we used the validation coefficient of determination ( $r^2$ ), root mean squared  
197 error of prediction (RMSE), and percent root mean squared error of prediction (%RMSE) as  
198 metrics to illustrate model fits.

199 To further evaluate the model performance, we used the model coefficients and variable  
200 influences on projection (VIP) values to explore the effect of different areas of the spectra on  
201 predicting the trait variable. Following this, we performed a jackknife permutation analysis to  
202 assess model uncertainty, using the jackknife argument of the ‘plsr’ function in the ‘pls’ R  
203 package [57]. The resulting jackknife coefficients were then compared to that of the full model.  
204 And finally, using the full model and jackknife permutation outputs, the mean, and 95%  
205 confidence and prediction intervals were calculated for each predicted trait value from the  
206 validation dataset.

207

## 208 **Results**

### 209 *Reflectance spectroscopy for predicting within-variety leaf traits*

210 Leaf traits measured here all varied significantly as a function of variety identity  
211 ( $p < 0.001$  in all cases). Specifically, across the entire dataset, physiological traits were most  
212 variable, with  $A_{\max}$  ranging from 3.8-29.0  $\mu\text{mol CO}_2 \text{ m}^{-2} \text{ s}^{-1}$  (CV=34.8),  $V_{\text{cmax}}$  from 28.9-131.7  
213  $\mu\text{mol m}^{-2} \text{ s}^{-1}$  (CV=27.5), and  $J_{\max}$  from 60.3-253.1  $\mu\text{mol m}^{-2} \text{ s}^{-1}$  (CV=25.8). In comparison, LMA  
214 and leaf N also varied significantly across varieties, though these traits were less variable with  
215 LMA ranging from 52.8-101.8  $\text{g m}^{-2}$  (CV=12.8) and leaf N from 2.04-4.39% (CV=13.7). All  
216 reflectance spectra presented generally the same shape, with a few Cab. Franc individuals

217 situated closer to the lower range, Merlot and Pinot Noir closer to the upper range, and others in  
218 and around the 95% confidence interval (Figure 1).

219 When calibration vs. validation data were evenly split across varieties (i.e., 80% of each  
220 variety allocated to each dataset), reflectance spectra and PLSR models explained between 18-  
221 64% of the variation in wine grape traits (Table 1, Figure 2). Specifically, physiological traits  
222 including  $A_{\max}$ ,  $J_{\max}$ , and  $V_{\max}$  were predicted by 4-5 spectral components which cumulatively  
223 explained 18%, 44%, and 30% of the variation in these traits, respectively. In these cases, model  
224 %RMSE values ranged from 21.6% in  $A_{\max}$  models, 24.1% in  $V_{\max}$  models, and 18.9% in  $J_{\max}$   
225 models. Comparatively, reflectance spectra and PLSR models expressed stronger predictive  
226 ability towards log-LMA and leaf N, with models ( $r^2$ ) explaining 64% (%RMSE=14.3) and 62%  
227 (%RMSE=15.2%) of the variation, respectively (Table 1, Figure 2).

228 The predictive power of PLSR models was sensitive to the configuration of calibration  
229 and validation datasets, though general trends were nuanced. When calibration and validation  
230 datasets were comprised of varieties in random proportions, physiological traits were better  
231 predicted than in datasets where variety proportions were equal. Specifically, in randomized data  
232 splits,  $A_{\max}$  model  $r^2=0.29$ ,  $V_{\max}$   $r^2=0.58$ , and  $J_{\max}$   $r^2=0.55$ , all of which were higher vs. the same  
233 models in variety-weighted data splits. Alternatively, PLSR models for log-LMA and leaf N had  
234 lower predictive power when calibration and validation datasets were randomly created, with  $r^2$   
235 values of 0.53 and 0.5, respectively (Table 1, Figure 2). In all cases, the number of spectral  
236 components retained in the final PLSR models also differed depending on the nature of  
237 calibration and validation dataset construction.

238 The impact of the data splitting method is also observed in the model regression  
239 coefficient trends, which reflect the contribution of certain wavelengths to trait prediction. For  
240 physiological traits, the shapes of regression coefficient trends are similar within the same  
241 splitting method, but distinctly different between splitting methods (Figure 3). Here we ignore  
242 the random split model of  $A_{\max}$  from this comparison, due to its limited number of model  
243 components. On the other hand, splitting data randomly or proportionally across varieties did not  
244 influence the regression coefficient distributions of log-LMA or leaf N (Figure 3). VIP scores of  
245 the models suggest similar wavelength regions of importance for model prediction across  
246 different traits, regardless of data splitting methods (Figure 4).

247



## 248 Discussion

249 Our findings contribute to the growing literature that reflectance spectroscopy is well-  
250 equipped to detect trait variation within and among plant species [27, 33, 35, 38, 40, 41, 45]. A  
251 considerable proportion of earlier work in this area focused on quantifying the interspecific trait  
252 variation that exists among plants of different functional types, that differ widely their  
253 evolutionary histories and trait diversity [e.g., 33, 35]. To this end, previous studies have  
254 indicated that reflectance spectroscopy is better equipped to explain trait variation, in situations  
255 where trait values within calibration and validation datasets vary more widely [38]. This  
256 tendency positions these techniques for rapid trait estimation in natural ecosystems [32], with  
257 many such studies reporting a high predictive ability of PLSR models in quantifying interspecific  
258 trait variation. Though a recent renewed focus on the importance of intraspecific trait variation in  
259 driving ecosystem functioning [20, 21], along with applications of these techniques in certain  
260 fields including agroecology, necessitates quantifying and disentangling the drivers of finer-scale  
261 trait variation that generally exists within species [24].

262 In this regard, our results show the strong predictive power of PLSR models to capture  
263 between 50-64% of the within-species trait variation in wine grapes, for key LES and related  
264 traits including  $V_{\text{cmax}}$ ,  $J_{\text{max}}$ , log-LMA, and leaf N (Table 1, Figure 2). Previous studies that  
265 examined within-species trait variation using PLSR approaches have yielded broadly similar  
266 results. For example, Meacham-Hensold et al. [46] reported PLSR models that explained 60%,  
267 59%, and 83% of the variation in  $V_{\text{cmax}}$ ,  $J_{\text{max}}$ , and leaf N, respectively, across six tobacco  
268 (*Nicotiana tabacum*) genotypes, though when three additional genotypes and larger sample sizes  
269 were included in analyses, these PLSR model  $r^2$  values increased to 0.61 for  $V_{\text{cmax}}$ , and 0.62 for  
270  $J_{\text{max}}$  in the validation dataset. Similarly, Fu et al. [47] modelled photosynthetic traits of six  
271 tobacco genotypes using PLSR methods, and reported similar  $r^2$  values (0.60 and 0.56) for  $V_{\text{cmax}}$   
272 and  $J_{\text{max}}$ , respectively.

273 Other single-species studies that applied reflectance spectroscopy and PLSR models to  
274 predict leaf traits across experimental treatments or environmental gradients have also presented  
275 similar results. For example, Yendrek et al. [43] found reflectance spectra were strong predictors  
276 of leaf N ( $r^2=0.92-0.96$ ) and  $V_{\text{cmax}}$  ( $r^2=0.56-0.65$ ) of maize (*Zea mays*) genotypes grown across  
277 gradients of ozone and soil N availability. Finally, in an analysis that screened over 200  
278 genotypes of wheat (*Triticum aestivum*, *T. turgidum*, and triticale germplasm) from six sets of

279 experiments, Silva-Perez et al. [42] included detected high predictive power of PLSR models,  
280 with  $r^2$  values ranging from 0.70-0.89 for leaf N, LMA,  $V_{\text{cmax}}$ , and  $J_{\text{max}}$ . Though in this same  
281 experiment, consistent with our results CO<sub>2</sub> assimilation rates were relatively poorly captured by  
282 PLSR models: in our analysis, the  $r^2$  for models for  $A_{\text{max}}$  were 0.18-0.29, vs.  $r^2$  values of 0.49 in  
283 Silva-Perez et al. [42].

284 In addition to model diagnostics alone, in our analysis, PLSR models generally support  
285 the same inferences surrounding the comparative trait biology of wine grape varieties (relative to  
286 observed trait data). Specifically, our previous analysis of LES trait variation—with trait data  
287 observed in the field using traditional gas exchange and analytical chemistry techniques—found  
288 that white grape varieties Sauvignon Blanc and Viognier occupy the “resource-acquiring” end of  
289 an intraspecific LES in wine grapes (characterized by high rates of  $A_{\text{max}}$ ,  $V_{\text{cmax}}$ ,  $J_{\text{max}}$ , leaf N, and  
290 low LMA), while red varieties (Cabernet Franc, Cabernet Sauvignon, Merlot) define the  
291 “resource-conserving” end of the wine grape LES (characterized by low  $A_{\text{max}}$ ,  $V_{\text{cmax}}$ ,  $J_{\text{max}}$ , leaf N,  
292 and high LMA). Our PLSR models support this same general trend (Figure 1), with white  
293 varieties expressing predictions that indicate resource-acquiring trait values.

294 Our analysis contributes evidence that reflectance spectroscopy and PLSR modelling  
295 approaches, can be used to 1) directly predict intraspecific trait variation with a relatively high  
296 degree of accuracy, and 2) differentiate intraspecific variation in life-history strategies in plants.  
297 Though our analysis here is based on a small subset of the 1,000s of wine grape varieties that  
298 exist globally [58]. Therefore, expanding this work to include a greater number of wine grape  
299 genotypes and trait values [cf. 41, 42], presents a viable opportunity to more rapidly screen trait  
300 expression in one of the world’s most economically important crops.

301

## 302 **Acknowledgments**

303 The authors acknowledge both Mitchell Madigan and Lauren Miller for their assistance with  
304 field data collection. This study was supported by a Discovery Grant to A.R.M. from the Natural  
305 Sciences and Engineering Research Council of Canada, and by the University of Toronto  
306 Scarborough’s (UTSC) Sustainable Food and Farming Futures (SF3) Cluster under UTSC’s  
307 Clusters of Scholarly Prominence Program.

308

## 309 **References**

- 310 1. Díaz S, Cabido M. Plant functional types and ecosystem function in relation to global  
311 change. *Journal of vegetation science*. 1997;8(4):463-74.
- 312 2. Funk JL, Larson JE, Ames GM, Butterfield BJ, Cavender-Bares J, Finn J, et al. Revisiting  
313 the Holy Grail: using plant functional traits to understand ecological processes. *Biological*  
314 *Reviews*. 2017;92(2):1156-73.
- 315 3. Lavorel S, Garnier E. Predicting changes in community composition and ecosystem  
316 functioning from plant traits: revisiting the Holy Grail. *Functional ecology*. 2002;16(5):545-56.
- 317 4. Westoby M, Wright IJ. Land-plant ecology on the basis of functional traits. *Trends in*  
318 *ecology & evolution*. 2006;21(5):261-8.
- 319 5. Díaz S, Hodgson J, Thompson K, Cabido M, Cornelissen JH, Jalili A, et al. The plant  
320 traits that drive ecosystems: evidence from three continents. *Journal of vegetation science*.  
321 2004;15(3):295-304.
- 322 6. Díaz S, Kattge J, Cornelissen JH, Wright IJ, Lavorel S, Dray S, et al. The global  
323 spectrum of plant form and function. *Nature*. 2016;529(7585):167-71.
- 324 7. Reich PB, Ellsworth DS, Walters MB, Vose JM, Gresham C, Volin JC, et al. Generality  
325 of leaf trait relationships: a test across six biomes. *Ecology*. 1999;80(6):1955-69.
- 326 8. Wright IJ, Reich PB, Cornelissen JH, Falster DS, Garnier E, Hikosaka K, et al. Assessing  
327 the generality of global leaf trait relationships. *New phytologist*. 2005;166(2):485-96.
- 328 9. Wright IJ, Reich PB, Westoby M, Ackerly DD, Baruch Z, Bongers F, et al. The  
329 worldwide leaf economics spectrum. *Nature*. 2004;428(6985):821-7.
- 330 10. Westoby M, Falster DS, Moles AT, Vesk PA, Wright IJ. Plant ecological strategies: some  
331 leading dimensions of variation between species. *Annual review of ecology and systematics*.  
332 2002;33(1):125-59.
- 333 11. Carmona CP, Bueno CG, Toussaint A, Träger S, Díaz S, Moora M, et al. Fine-root traits  
334 in the global spectrum of plant form and function. *Nature*. 2021;597(7878):683-7.
- 335 12. Shipley B, Lechowicz MJ, Wright I, Reich PB. Fundamental trade-offs generating the  
336 worldwide leaf economics spectrum. *Ecology*. 2006;87(3):535-41.
- 337 13. Blonder B, Violle C, Bentley LP, Enquist BJ. Venation networks and the origin of the  
338 leaf economics spectrum. *Ecology letters*. 2011;14(2):91-100.
- 339 14. Xiong D, Flexas J. Leaf economics spectrum in rice: leaf anatomical, biochemical, and  
340 physiological trait trade-offs. *Journal of Experimental Botany*. 2018;69(22):5599-609.
- 341 15. Onoda Y, Wright IJ, Evans JR, Hikosaka K, Kitajima K, Niinemets Ü, et al.  
342 Physiological and structural tradeoffs underlying the leaf economics spectrum. *New Phytologist*.  
343 2017;214(4):1447-63.
- 344 16. Onoda Y, Wright IJ. The leaf economics spectrum and its underlying physiological and  
345 anatomical principles. *The leaf: a platform for performing photosynthesis*. 2018:451-71.
- 346 17. Anderegg LD, Berner LT, Badgley G, Sethi ML, Law BE, HilleRisLambers J.  
347 Within-species patterns challenge our understanding of the leaf economics spectrum. *Ecology*  
348 *letters*. 2018;21(5):734-44.
- 349 18. Bolnick DI, Amarasekare P, Araújo MS, Bürger R, Levine JM, Novak M, et al. Why  
350 intraspecific trait variation matters in community ecology. *Trends in ecology & evolution*.  
351 2011;26(4):183-92.
- 352 19. Violle C, Enquist BJ, McGill BJ, Jiang L, Albert CH, Hulshof C, et al. The return of the  
353 variance: intraspecific variability in community ecology. *Trends in ecology & evolution*.  
354 2012;27(4):244-52.

- 355 20. Westerband A, Funk J, Barton K. Intraspecific trait variation in plants: a renewed focus  
356 on its role in ecological processes. *Annals of botany*. 2021;127(4):397-410.
- 357 21. Siefert A, Violle C, Chalmandrier L, Albert CH, Taudiere A, Fajardo A, et al. A global  
358 meta-analysis of the relative extent of intraspecific trait variation in plant communities. *Ecology*  
359 *letters*. 2015;18(12):1406-19.
- 360 22. Isaac ME, Martin AR, de Melo Virginio Filho E, Rapidel B, Roupsard O, Van den  
361 Meersche K. Intraspecific trait variation and coordination: Root and leaf economics spectra in  
362 coffee across environmental gradients. *Frontiers in plant science*. 2017;8:1196.
- 363 23. Milla R, Osborne CP, Turcotte MM, Violle C. Plant domestication through an ecological  
364 lens. *Trends in ecology & evolution*. 2015;30(8):463-9.
- 365 24. Martin AR, Isaac ME. Plant functional traits in agroecosystems: a blueprint for research.  
366 *Journal of Applied Ecology*. 2015;52(6):1425-35.
- 367 25. Saathoff AJ, Welles J. Gas exchange measurements in the unsteady state. *Plant, Cell &*  
368 *Environment*. 2021;44(11):3509-23.
- 369 26. Reich P, Ellsworth D, Walters M. Leaf structure (specific leaf area) modulates  
370 photosynthesis–nitrogen relations: evidence from within and across species and functional  
371 groups. *Functional Ecology*. 1998;12(6):948-58.
- 372 27. Serbin SP, Wu J, Ely KS, Kruger EL, Townsend PA, Meng R, et al. From the Arctic to  
373 the tropics: multibiome prediction of leaf mass per area using leaf reflectance. *New Phytologist*.  
374 2019;224(4):1557-68.
- 375 28. Fahlgren N, Gehan MA, Baxter I. Lights, camera, action: high-throughput plant  
376 phenotyping is ready for a close-up. *Current opinion in plant biology*. 2015;24:93-9.
- 377 29. Asner GP, Martin RE, Anderson CB, Knapp DE. Quantifying forest canopy traits:  
378 Imaging spectroscopy versus field survey. *Remote Sensing of Environment*. 2015;158:15-27.
- 379 30. Singh A, Serbin SP, McNeil BE, Kingdon CC, Townsend PA. Imaging spectroscopy  
380 algorithms for mapping canopy foliar chemical and morphological traits and their uncertainties.  
381 *Ecological Applications*. 2015;25(8):2180-97.
- 382 31. Chadwick KD, Brodrick PG, Grant K, Goulden T, Henderson A, Falco N, et al.  
383 Integrating airborne remote sensing and field campaigns for ecology and Earth system science.  
384 *Methods in Ecology and Evolution*. 2020;11(11):1492-508.
- 385 32. Asner GP, Knapp DE, Anderson CB, Martin RE, Vaughn N. Large-scale climatic and  
386 geophysical controls on the leaf economics spectrum. *Proceedings of the National Academy of*  
387 *Sciences*. 2016;113(28):E4043-E51.
- 388 33. Serbin SP, Singh A, McNeil BE, Kingdon CC, Townsend PA. Spectroscopic  
389 determination of leaf morphological and biochemical traits for northern temperate and boreal tree  
390 species. *Ecological Applications*. 2014;24(7):1651-69.
- 391 34. Serbin SP, Dillaway DN, Kruger EL, Townsend PA. Leaf optical properties reflect  
392 variation in photosynthetic metabolism and its sensitivity to temperature. *Journal of*  
393 *Experimental Botany*. 2012;63(1):489-502.
- 394 35. Kothari S, Beauchamp-Rioux R, Blanchard F, Crofts AL, Girard A, Guilbeault-Mayers  
395 X, et al. Predicting leaf traits across functional groups using reflectance spectroscopy. *New*  
396 *Phytologist*. 2023;238(2):549-66.
- 397 36. Burnett AC, Anderson J, Davidson KJ, Ely KS, Lamour J, Li Q, et al. A best-practice  
398 guide to predicting plant traits from leaf-level hyperspectral data using partial least squares  
399 regression. *Journal of Experimental Botany*. 2021;72(18):6175-89.

- 400 37. Dechant B, Cuntz M, Vohland M, Schulz E, Doktor D. Estimation of photosynthesis  
401 traits from leaf reflectance spectra: Correlation to nitrogen content as the dominant mechanism.  
402 Remote Sensing of Environment. 2017;196:279-92.
- 403 38. Lamour J, Davidson KJ, Ely KS, Anderson JA, Rogers A, Wu J, et al. Rapid estimation  
404 of photosynthetic leaf traits of tropical plants in diverse environmental conditions using  
405 reflectance spectroscopy. Plos one. 2021;16(10):e0258791.
- 406 39. Doughty CE, Santos-Andrade P, Goldsmith G, Blonder B, Shenkin A, Bentley L, et al.  
407 Can leaf spectroscopy predict leaf and forest traits along a Peruvian tropical forest elevation  
408 gradient? Journal of Geophysical Research: Biogeosciences. 2017;122(11):2952-65.
- 409 40. Ely KS, Burnett AC, Lieberman-Cribbin W, Serbin SP, Rogers A. Spectroscopy can  
410 predict key leaf traits associated with source–sink balance and carbon–nitrogen status. Journal of  
411 experimental botany. 2019;70(6):1789-99.
- 412 41. Vasseur F, Cornet D, Beurier G, Messier J, Rouan L, Bresson J, et al. A perspective on  
413 plant phenomics: coupling deep learning and near-infrared spectroscopy. Frontiers in Plant  
414 Science. 2022;13:836488.
- 415 42. Silva-Perez V, Molero G, Serbin SP, Condon AG, Reynolds MP, Furbank RT, et al.  
416 Hyperspectral reflectance as a tool to measure biochemical and physiological traits in wheat.  
417 Journal of Experimental Botany. 2018;69(3):483-96.
- 418 43. Yendrek CR, Tomaz T, Montes CM, Cao Y, Morse AM, Brown PJ, et al. High-  
419 throughput phenotyping of maize leaf physiological and biochemical traits using hyperspectral  
420 reflectance. Plant physiology. 2017;173(1):614-26.
- 421 44. Heckmann D, Schlüter U, Weber AP. Machine learning techniques for predicting crop  
422 photosynthetic capacity from leaf reflectance spectra. Molecular plant. 2017;10(6):878-90.
- 423 45. Burnett AC, Serbin SP, Rogers A. Source: sink imbalance detected with leaf-and  
424 canopy-level spectroscopy in a field-grown crop. Plant, Cell & Environment. 2021;44(8):2466-  
425 79.
- 426 46. Meacham-Hensold K, Montes CM, Wu J, Guan K, Fu P, Ainsworth EA, et al. High-  
427 throughput field phenotyping using hyperspectral reflectance and partial least squares regression  
428 (PLSR) reveals genetic modifications to photosynthetic capacity. Remote Sensing of  
429 Environment. 2019;231:111176.
- 430 47. Fu P, Meacham-Hensold K, Guan K, Wu J, Bernacchi C. Estimating photosynthetic traits  
431 from reflectance spectra: a synthesis of spectral indices, numerical inversion, and partial least  
432 square regression. Plant, Cell & Environment. 2020;43(5):1241-58.
- 433 48. Macklin SC, Mariani RO, Young EN, Kish R, Cathline KA, Robertson G, et al.  
434 Intraspecific leaf trait variation across and within five common wine grape varieties. Plants.  
435 2022;11(20):2792.
- 436 49. Martin AR, Mariani RO, Cathline KA, Duncan M, Paroshy NJ, Robertson G. Soil  
437 compaction drives an intra-genotype leaf economics spectrum in wine grapes. Agriculture.  
438 2022;12(10):1675.
- 439 50. Perez-Harguindeguy N, Diaz S, Garnier E, Lavorel S, Poorter H, Jaureguiberry P, et al.  
440 Corrigendum to: New handbook for standardised measurement of plant functional traits  
441 worldwide. Australian Journal of botany. 2016;64(8):715-6.
- 442 51. Gregory LM, Roze LV, Walker BJ. Increased activity of core photorespiratory enzymes  
443 and CO<sub>2</sub> transfer conductances are associated with higher and more optimal photosynthetic rates  
444 under elevated temperatures in the extremophile *Rhazya stricta*. Plant, Cell & Environment.  
445 2023;46(12):3704-20.

- 446 52. McClain AM, Sharkey TD. Rapid CO<sub>2</sub> changes cause oscillations in photosynthesis that  
447 implicate PSI acceptor-side limitations. *Journal of Experimental Botany*. 2023;74(10):3163-73.  
448 53. Stinziano JR, McDermitt DK, Lynch DJ, Saathoff AJ, Morgan PB, Hanson DT. The  
449 rapid A/C i response. *New Phytologist*. 2019;221(2):625-7.  
450 54. Duursma RA. Plantecophys-an R package for analysing and modelling leaf gas exchange  
451 data. *PloS one*. 2015;10(11):e0143346.  
452 55. Delignette-Muller ML, Dutang C. fitdistrplus: An R package for fitting distributions.  
453 *Journal of statistical software*. 2015;64:1-34.  
454 56. Lamour J, Serbin S. spectratrait: A simple add-on package to aid in the fitting of leaf-  
455 level spectra-trait PLSR models. In: 1.2.1 Rpv, editor. 2023.
- 456 57. Liland K, Mevik B, Wehrens R. pls: Partial Least Squares and Principal Component  
457 Regression. In: 2.8-1 Rpv, editor. 2022.
- 458 58. Wolkovich E, García de Cortázar-Atauri I, Morales-Castilla I, Nicholas K, Lacombe T.  
459 From Pinot to Xinomavro in the world's future wine-growing regions. *Nature Climate Change*.  
460 2018;8(1):29-37.

461

462 **Tables and Figures**

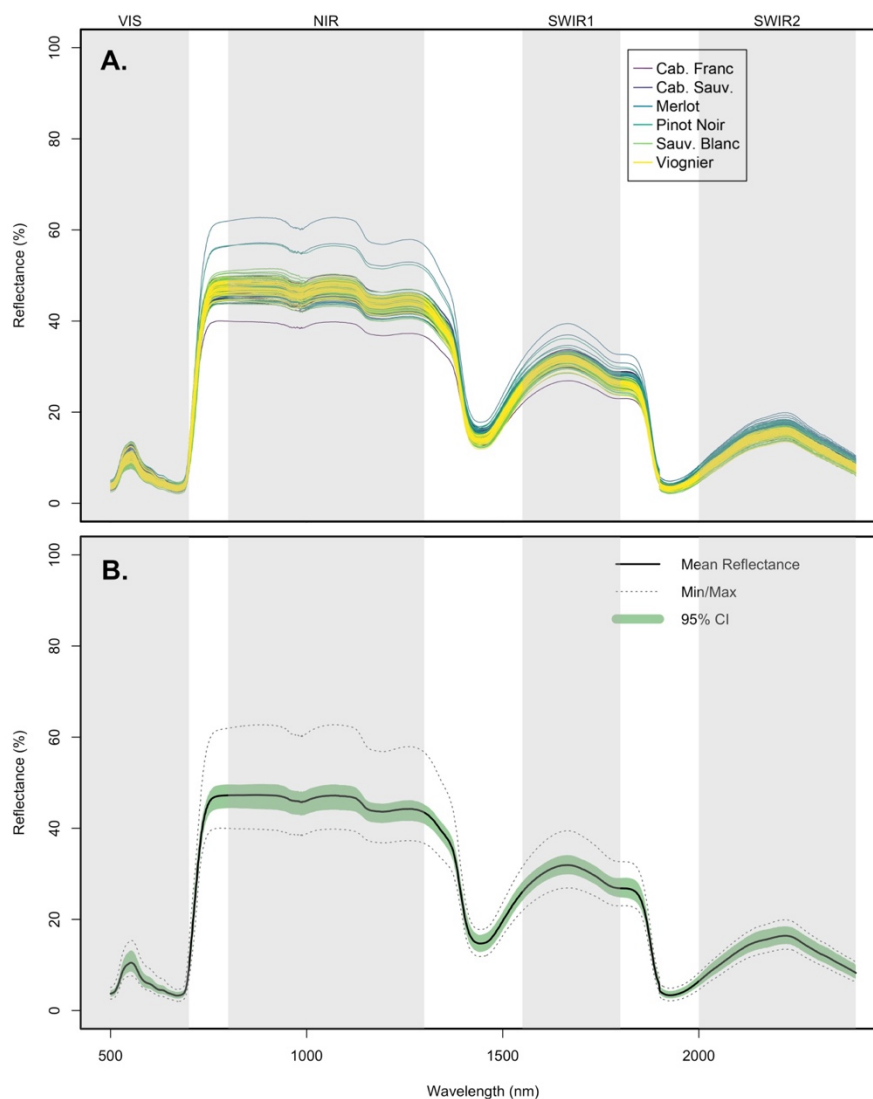
463

464 **Table 1.** Partial least squares regression model fits evaluating the ability of reflectance spectra to  
465 explain variation in leaf traits measured on six wine grape varieties. Presented here are results  
466 from two different modelling approaches which divide our total sample into calibration (80% of  
467 our data) vs. validation (20% of our data) datasets. In the results associated with the “Variety”  
468 approach, calibration and validation data both included approximately the same proportions of  
469 observations from all varieties, while the “Random” approach made this division randomly.  
470 Here,  $n_{\text{obs}}$  refers to the total observations in our dataset for a given trait, which entails a  
471 correspond sample size in the validation dataset ( $n_{\text{val}}$ ). For each model we present the number of  
472 components derived from reflectance spectra that were included in the final predictive model  
473 ( $n_{\text{comp}}$ ), along with the root mean square error (RMSE),  $r^2$  value, and %RMSE for the final  
474 predictive model. All models were based on Trait acronyms are as follows: light saturated  
475 photosynthetic rate ( $A_{\text{max}}$ ), maximum velocity of Ribulose 1,5-bisphosphate (RuBP)  
476 carboxylation ( $V_{\text{cmax}}$ ), maximum rate of electron transport ( $J_{\text{max}}$ ), leaf mass per area (LMA), leaf  
477 nitrogen (N) concentration.

478

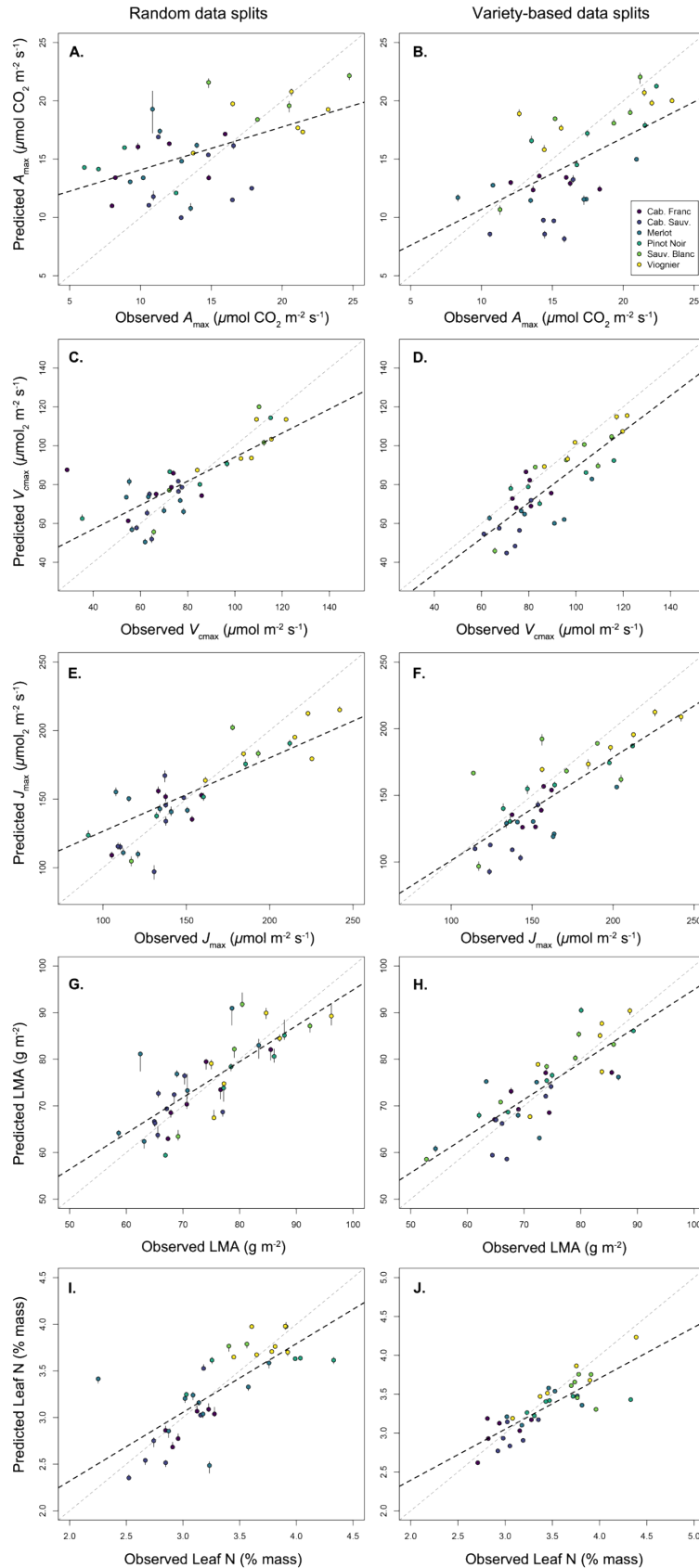
| Data split | Trait             | $n_{\text{obs}}$ | $n_{\text{val}}$ | $n_{\text{comp}}$ | RMSE  | $r^2$ | %RMSE |
|------------|-------------------|------------------|------------------|-------------------|-------|-------|-------|
| Variety    | $A_{\text{max}}$  | 178              | 36               | 4                 | 3.9   | 0.18  | 21.63 |
|            | $V_{\text{cmax}}$ | 177              | 36               | 5                 | 14.62 | 0.3   | 24.1  |
|            | $J_{\text{max}}$  | 177              | 36               | 4                 | 24.22 | 0.44  | 18.88 |
|            | log-LMA           | 178              | 36               | 10                | 0.08  | 0.64  | 14.27 |
|            | Leaf N            | 176              | 36               | 9                 | 0.25  | 0.62  | 15.16 |
| Random     | $A_{\text{max}}$  | 178              | 36               | 1                 | 4.42  | 0.29  | 19.25 |
|            | $V_{\text{cmax}}$ | 177              | 36               | 9                 | 14.47 | 0.58  | 15.6  |
|            | $J_{\text{max}}$  | 177              | 36               | 8                 | 28.35 | 0.55  | 15.6  |
|            | log-LMA           | 178              | 36               | 13                | 0.08  | 0.53  | 16.44 |
|            | Leaf N            | 176              | 36               | 11                | 0.33  | 0.5   | 15.92 |

479

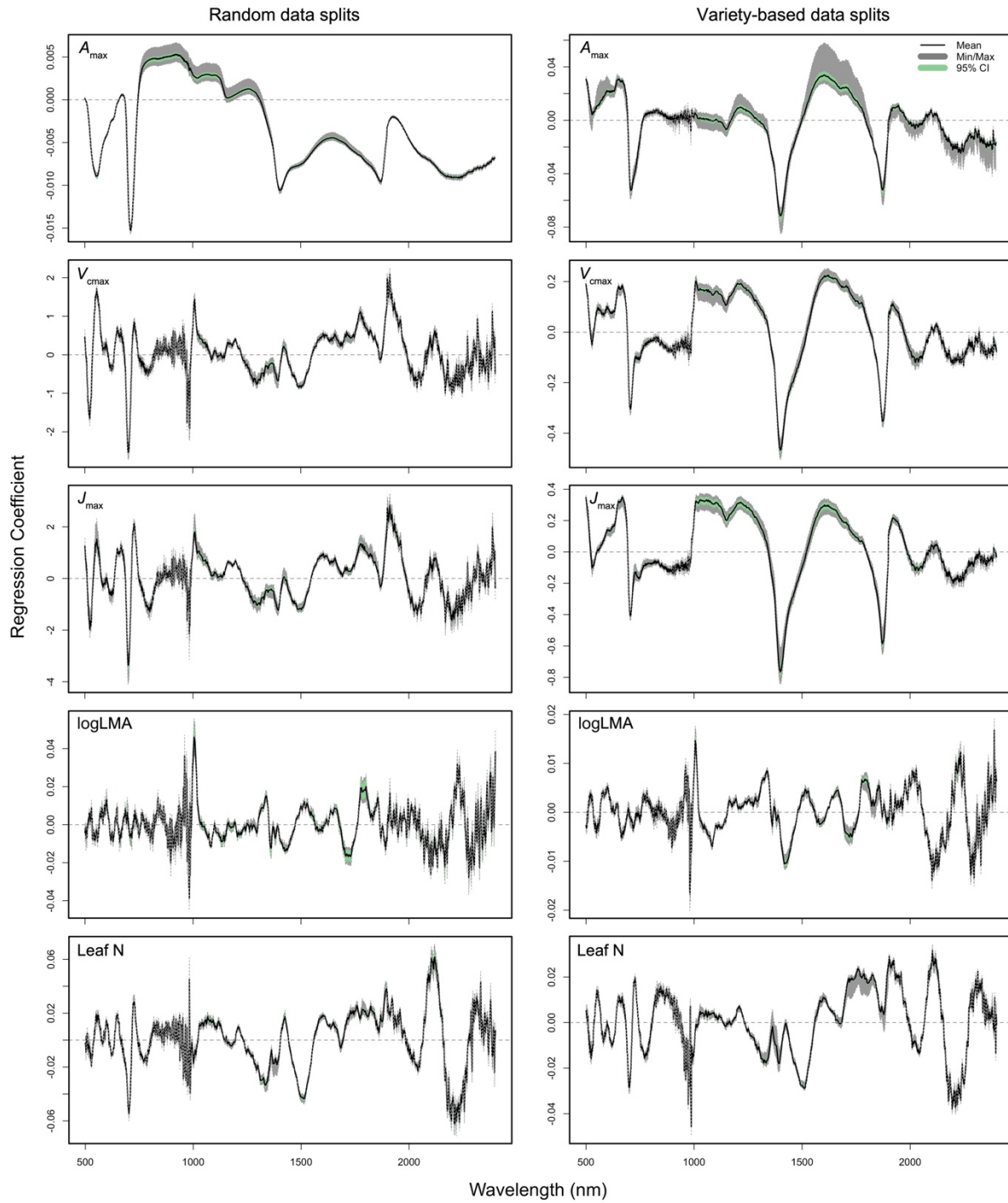


480  
481 **Figure 1.** Reflectance spectra of 179 wine grape leaves plotted A) individually with six wine  
482 grape varieties specified, and B) all together with mean, range, and 95% confidence interval  
483 estimates. All spectral data were trimmed to the 500-2400 nm range where the PLSR models  
484 were built from. The grey shaded areas indicate different spectral regions: Visible Spectrum  
485 (VIS), Near Infrared (NIR), Short Wave Infrared 1 (SWIR1), and Short Wave Infrared 2  
486 (SWIR2).





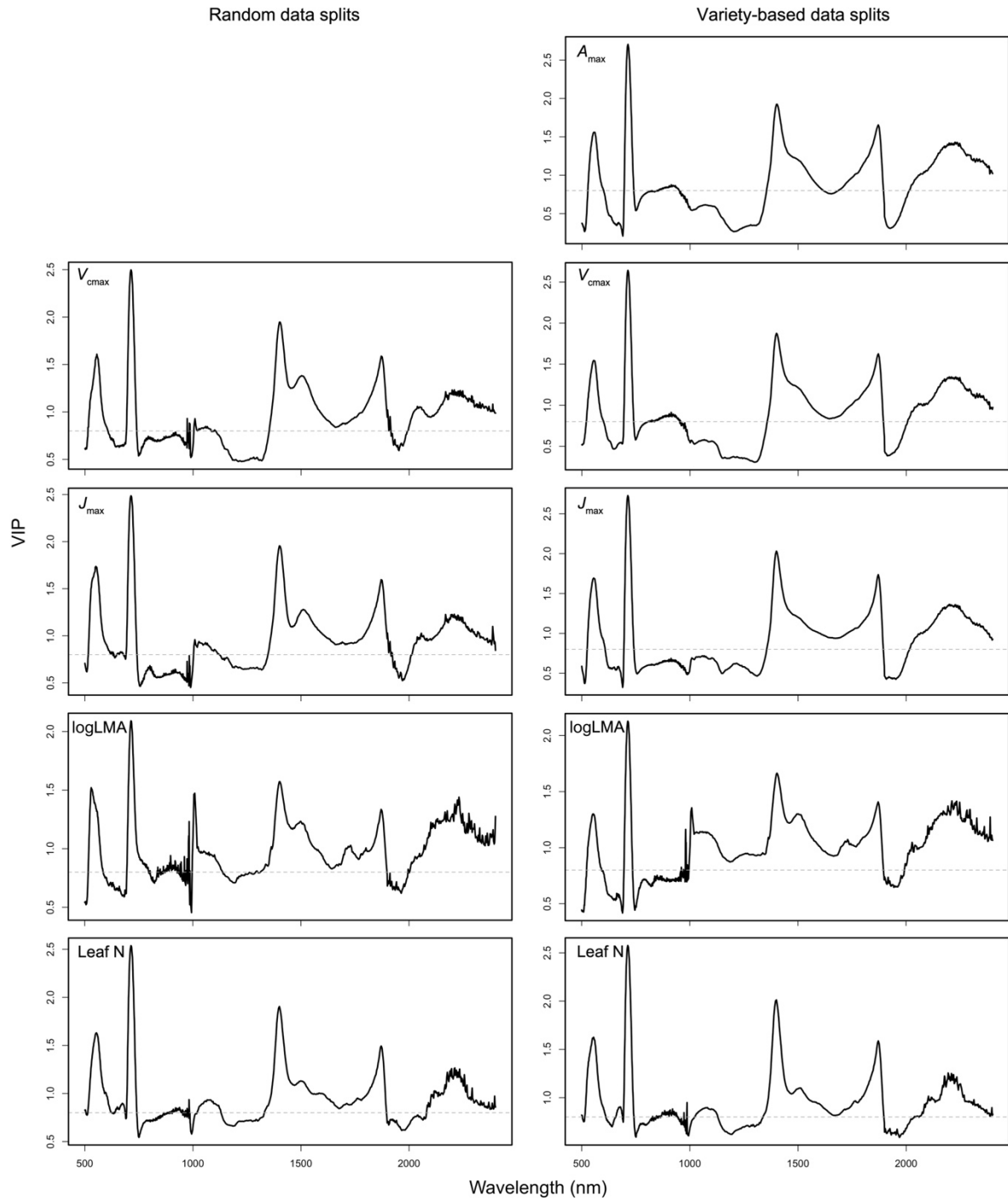
488 **Figure 2.** Results of partial least squares regression (PLSR) models predicting leaf physiological,  
489 chemical, and morphological traits in six wine grape varieties. Shown here are the data points  
490 used to validate the models ( $n=36$  in all cases) fitted to a set of calibration data points ( $n=176$ -  
491 178; see Table 1). Calibration and validation datasets were selected on the basis of a fully  
492 randomized data split (left panels), and a data split where all six varieties were equally  
493 represented in the calibration datasets (right panels). Dashed black lines represent linear model  
494 fits between observed vs. expected trait values, while the dotted gray lines represent a 1:1  
495 relationship.



497 **Figure 3.** Jackknife regression coefficients of the PLSR models of  $A_{\max}$ ,  $V_{\text{cmax}}$ ,  $J_{\max}$ , log-LMA,  
498 and leaf N, based on the calibration data. The dashed horizontal line in each panel indicates  
499 where the coefficient is zero. The black curve represents the mean, the grey area represents the  
500 range, and the green area represents the 95% confidence interval.

501

502



503

504 **Figure 4.** Variable influences on projection (VIP) scores of the final PLSR models of  $A_{\max}$ ,  
505  $V_{\text{cmax}}$ ,  $J_{\text{max}}$ , log-LMA, and leaf N. The dashed horizontal line in each panel indicates where the  
506 VIP score is 0.8. The  $A_{\text{max}}$  model using random data split method had one component and  
507 therefore did not generate valid VIP scores.